



Original papers

A new approach for estimating mangrove canopy cover using Landsat 8 imagery

Hesham Abd-El Monsef^{a,*}, Scot E. Smith^b^a Suez Canal University, Faculty of Science, Geology Department, Ismailia, Egypt^b Geomatics Program, University of Florida, Gainesville, FL, USA

ARTICLE INFO

Article history:

Received 4 June 2016

Received in revised form 7 February 2017

Accepted 9 February 2017

Available online 17 February 2017

Keywords:

Landsat 8

Mangrove

Normalized Difference Vegetation Index

Infrared Index

Leaf Area Index

Green Atmospherically Resistant Index

Optimized Soil Adjusted Vegetation Index

Normalized Difference Built-up Index

Normalized Difference Water Index

ABSTRACT

Due to background reflectance, it is difficult to accurately map sparse canopy vegetation using moderate-resolution satellite imagery. Information contained in virtually all the pixels is a mix of leaf vegetation, soil, branches and shadow. Presented in this paper is a novel approach to improving the accuracy of mapping mangrove canopy using Landsat 8 imagery by incorporating seven indices: Normalized Difference Vegetation Index, Infrared Index, Leaf Area Index, Green Atmospherically Resistant Index, Optimized Soil Adjusted Vegetation Index, Normalized Difference Built-up Index and Normalized Difference Water Index. Results demonstrated that the accuracy of mapping mangrove can be significantly improved using this approach.

© 2017 Elsevier B.V. All rights reserved.

1. Introduction

Fragile ecosystems, such as mangroves, require continuous monitoring to detect threats, including human activities, pollution, over-grazing, disease, fire, storms and desiccation. A monitoring system is also needed for mangrove plantations as it provides empirical data for measuring the rate of growth and identifies areas needing remedial attention.

Canopy cover is an indicator of the status of mangrove stands and it is an indicator useful for assessing the impact of deleterious pressure factors on mangroves. Therefore, a method to accurately estimate mangrove canopy cover is needed for monitoring.

The study area was the southern-most mangrove stand in the Abu Hamrah al Bahray Bay located along the Egyptian Red Sea coast as shown in Fig. 1. Two Landsat 8 scenes, dated 29 June and 6 July 2013, were used. The area on 6 July 2013 is shown in Fig. 2.

The mangrove stands of Abu Hamrah al Bahray stands extend 1 km with a width ranging from 50 m to 140 m. They have a total area of approximately 68,000 square meters. The mangroves can

be subdivided into north, middle and south stands. The south stand faces the sea and grows over two horseshoe shaped sand bars. Individual mangrove trees are located in the front part of the horseshoe. The middle stand is a small bay with soil enriched by fine black detritus. The bay is connected to the north strand via a narrow channel which is 8–11 m wide. The north strand is an elongated inland creek that is 360 m long and 60 m wide.

Landsat 8 images are free-of-charge online, while other earth remote sensing satellite imagery such as RapidEye, WorldView, QuickBird or GeoEye cost several thousand dollars per square kilometer. Landsat 8 provides the multispectral bands necessary for the majority of vegetation indices. The revisit time of Landsat 8 is eight days so that monitoring can be done frequently. In contrast, most earth remote sensing satellite systems require pre-acquisition ordering and so the number of images for any particular site is low.

The downside of Landsat 8 is that, due to an instantaneous field of view (IFOV) of 30 m × 30 m, while some of the area within the IFOV will be vegetation, some will be sand, shadow, dead branches and detritus. These "mixed pixels" result in inaccurate classification because they do not represent a homogeneous land cover type. The research in this paper shows a technique to overcome that problem.

* Corresponding author.

E-mail addresses: Hesham_geo@yahoo.com (H.A.-E. Monsef), Sesmith@ufl.edu (S.E. Smith).

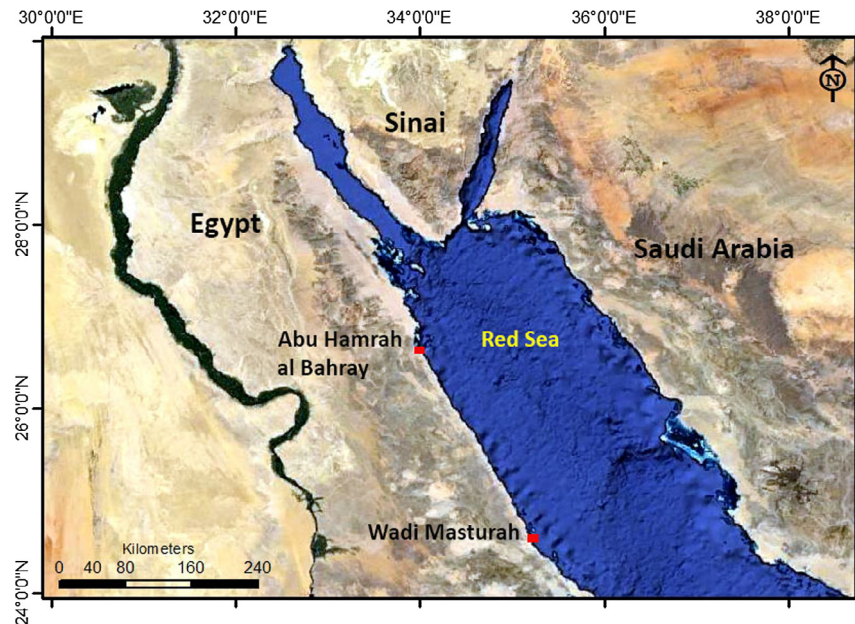


Fig. 1. Landsat 8 scene study area on 6 July 2013.

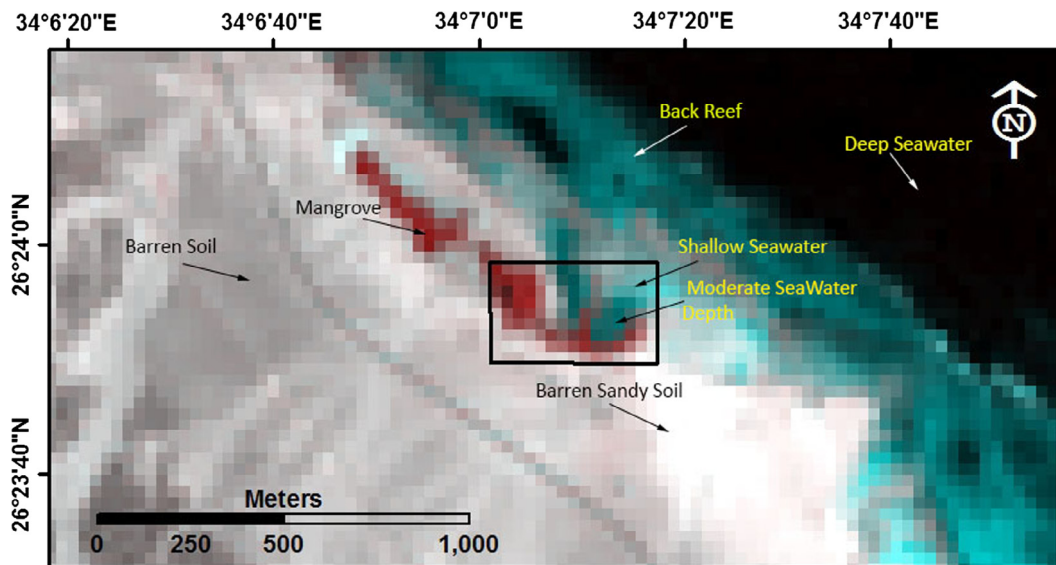


Fig. 2. Landsat 8 image of study area. Mangrove stands are in red. (For interpretation of the references to colour in this figure legend, the reader is referred to the web version of this article.)

The Normalized Difference Vegetation Index (NDVI) is commonly used for vegetation monitoring systems, but imagery is costly because it works best with very high spatial resolution (i.e., 1 m) satellite images such as WorldView, QuickBird or GeoEye. The high spatial resolution imagery is needed to get a nearly “pure IFOVs” with a spectral characteristic affected only by the vegetation and not mixed with other reflectance's.

The ideal condition is when each IFOV of the image can be assigned to a single spectrally homogeneous land cover type. However, satellite images such as Landsat 8, with a 30 m × 30 m IFOV, this condition is rarely found in nature. Mangrove stands usually have a small areal extent and consist of widely dispersed patches of trees. Therefore, the 30 m by 30 m IFOV usually includes more than one type of land cover. The measured spectral radiance of an IFOV is the integration of the radiance reflected from all the area

within the IFOV and so data in an IFOV is from a mixture of land cover types. In order to accurately identify the mangrove canopy, the percent of it in each image IFOV needs to be estimated. Spectral unmixing is based on the assumption that several primitive classes or endmembers of interest can be selected. Each have primitive classes has a pure spectral signature which can be identified and the mixing between these classes can be adequately modelled as a linear combination of the spectral signatures (Small, 2004).

The spectral signature of an object can be defined as the amount of electromagnetic radiation emitted, reflected or absorbed at varying wavelengths from an object. The accuracy of unmixing process is affected by many factors, including atmosphere attenuation, scattering, terrain and similarity between the object spectral signatures. In this study, we overcame these problems with the unmixing process by using band indices instead of spectral bands

to construct a spectral signature of the study area's land cover. By using indices, one still uses the same assumption of spectral unmixing since the value of an IFOV in each index layer is a contribution of the index values of its surface land cover types.

2. Methods

The method used in this study is shown in a flow chart (Fig. 3). Our objective was to estimate mangrove canopy cover using Landsat 8 imagery.

2.1. Image preparation

Two Landsat 8 scenes, dated 17 and 24 June 2013, were used. Twenty-five image identifiable Ground Control Points (GCPs) were selected. Field work was performed in order to verify the coordinates of GCPs using Differential Global Positioning System (DGPS) with sub-meter accuracy. Eventually, these ground control points were used to geometrically rectify the images.

Landsat 8 imagery has with metadata file stores spectral band gain and offset numbers that can be used to linearly convert the

digital numbers to at-sensor radiance ($\text{W m}^{-2} \text{sr}^{-1} \mu\text{m}^{-1}$) and to convert the OLI digital numbers to at-sensor reflectance. In this research the "Radiometric Calibration" module of ENVI 5.3 software was utilized to calibrate the imagery by using Fast Line-of-sight Atmospheric Analysis of Hypercubes (FLAASH). FLAASH is a first-principle atmospheric correction tool that corrects wavelengths in the visible through near-infrared and shortwave infrared regions of the electromagnetic spectrum.

2.2. Construction of the seven index image

For mapping vegetation, vegetation indices are usually used separately. This research designed and implemented a new approach to integrate several vegetation indices to map vegetation. The type and number of indices in the approach depended on the (1) condition of the study area, (2) vegetation type, (3) vegetation density and (4) the task of the demarcation or inventory process. In this study, seven vegetation indices were selected for the demarcation and inventory of mangroves growing in arid condition such as the Red Sea. These indices were selected to cover dominant factors controlling vegetation's reflectance in addition to the background (sand, branches, shadow and detritus):

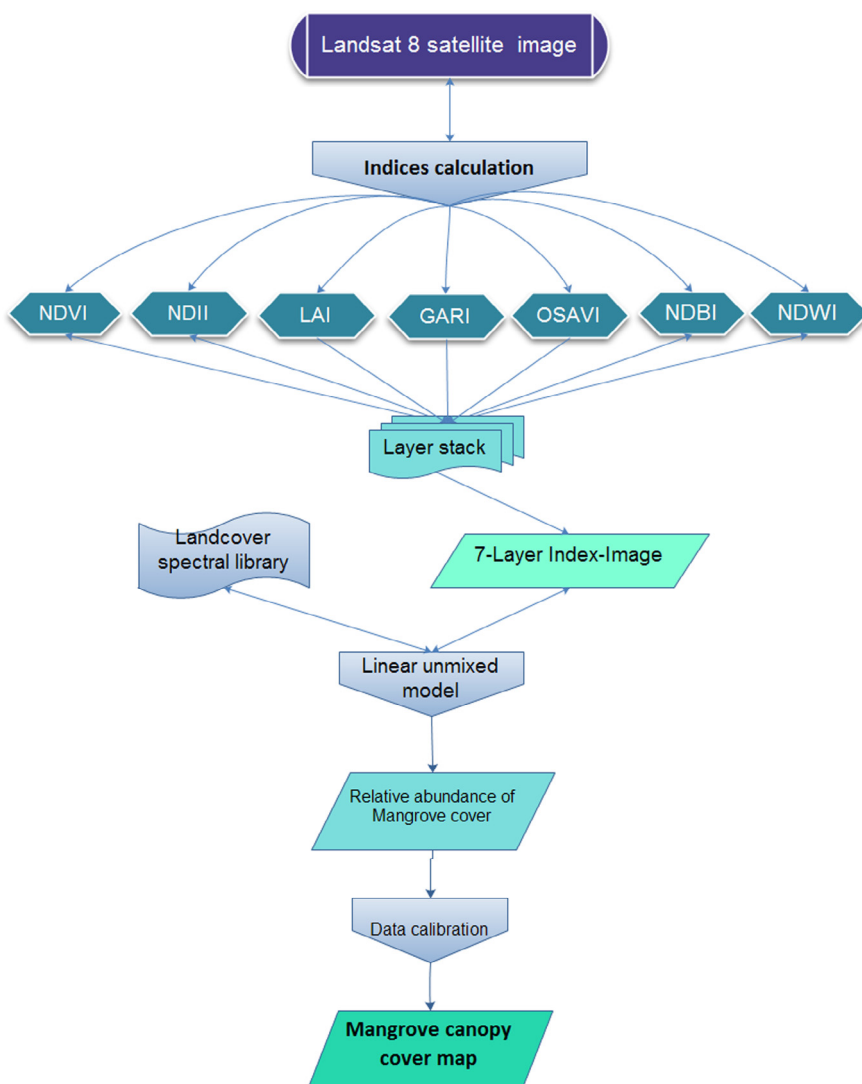


Fig. 3. Approach used to estimate mangrove canopy cover using Landsat 8 imagery.

- a. Visible Light Interaction with Pigments in Palisade Mesophyll Cells.
 - o Green Atmospherically Resistant Index (GARI) is sensitive to a wide range of chlorophyll concentrations (Gitelson et al., 1996).
- b. Near-Infrared Energy Interaction with Spongy Mesophyll Cells.
 - o Normalized Difference Vegetation Index (NDVI) depends on the inverse relationship between red and near-infrared reflectance associated with healthy green vegetation. This means that the NDVI depends on the status of the chlorophyll content and the spongy cells (Rouse et al., 1974).
- c. Mid-infrared Energy Interaction with Water in Spongy Mesophyll Cells.
 - o Normalized Difference Water Index (NDWI) is a measure of vegetation water content (Sims and Gamon, 2003).
 - o Normalized Difference Infrared Index (NDII) is sensitive to changes in plant biomass and water stress.
- d. Background soil.
 - o Normalized Difference Built-up Index (NDBI) is useful in separating bare soil from vegetated land (Zha et al., 2003).
 - o Optimized Soil Adjusted Vegetation Index (OSAVI), in conjunction with the NDVI, LAI and GARI, reduces the soil background effect (Rondeaux et al., 1996).
 - o Leaf Area Index (LAI) is vegetation density. In reverse, it is a measure of the area of background reflectance (Green et al., 2014).

Sand is the main factor affecting the accuracy of mangrove classification due to the low density of the mangroves. Therefore, three indices that take into consideration the sand were used. We used the three indices (NDBI, OSAVI and LAI) to be certain that the sand effect was treated properly before applying unmixing analysis.

2.2.1. Green Atmospherically Resistant Index (GARI)

The Atmospherically Resistant Index (GARI) is used to detect and differentiate a wide range of green pigment concentration. GARI is more sensitive to a wide range of chlorophyll concentrations and less sensitive to atmospheric effects than NDVI (Gitelson et al., 1996). GARI is calculated using the following equation:

$$GARI = \frac{NIR - (Green - 1.7^*(Blue - Red))}{NIR + (Green - 1.7^*(Blue - Red))} \quad (1)$$

2.2.2. Normalized Difference Vegetation Index (NDVI)

The NDVI is widely used to map vegetation, it is calculated by rationing near-infrared radiation minus red light by near-infrared radiation plus red light as shown in Eq. (2):

$$NDVI = \frac{(NIR - R)}{(NIR + R)} \quad (2)$$

where, NIR is the near infrared band, R is the red band.

2.2.3. Normalized Difference Water Index (NDWI)

Sims and Gamon (2003) found that the normalized difference water index (NDWI) was a good water absorption index for comparison with NDVI for the application of monitoring live fuel moisture. NDWI is calculated as:

$$NDWI = \frac{Green - NIR}{Green + NIR} \quad (3)$$

The NDWI (Fig. 6) was designed to maximize water reflection in green light and minimize reflectance in NIR. Hence using NDWI with NDVI takes advantage of the high reflectance of NIR by vegetation and enhances the differentiation between water bodies, wetland and vegetation.

2.2.4. Normalized Difference Infrared Index (NDII)

Hardisky et al. (1983) found that the Normalized Difference Infrared Index (NDII), based on Landsat near- and mid-infrared bands, was more sensitive to changes in plant biomass and water stress than NDVI for wetland vegetation such as mangroves. The equation used to calculate NDII for Landsat 8 is:

$$NDII = \frac{NIR_{B5} - MidIR_{B6}}{NIR_{B5} + MidIR_{B6}} \quad (4)$$

where, NIR_{B5} and $MidIR_{B6}$ are band 5 and band 6, respectively, of Landsat 8.

Although the NDII was designed to measure the vegetation's water content, it is useful to differentiate between dry soil and soil with different moisture content and water bodies of different depths. For instance, dry sand has a very low NDII because NIR and MidIR are both highly reflected by dry sand. This leads to a high ratio for the NDII equation.

2.2.5. Normalized Difference Built-up Index (NDBI)

Although the NDBI was developed originally for monitoring the spatial distribution and growth of urban areas, it is found useful in separating barren soil from vegetated land.

The NDBI can be calculated using Eq. (5) (Zha et al., 2003). Fig. 8 is an image from the NDBI of the study area:

$$NDBI = \frac{MidIR_{Band6} - NIR}{MidIR_{Band6} + NIR} \quad (5)$$

2.2.6. Optimized Soil Adjusted Vegetation Index (OSAVI)

Using OSAVI in conjunction with the NDVI, LAI and GARI reduces the soil background effect (Rondeaux et al., 1996). The OSAVI is calculated using Eq. (6).

$$OSAVI = \frac{1.5^*(NIR - Red)}{(NIR + Red + 0.16)} \quad (6)$$

2.2.7. Leaf Area Index (LAI)

The LAI is used to estimate foliage cover and to forecast crop growth and yield. LAI is the fraction of direct solar radiation that penetrates the canopy. It is the ratio between the light flux density beneath the canopy (L_c) and the light flux density outside the canopy (L_o). LAI can then be calculated and corrected for sun angle from zenith using the formula devised by English et al. (1997):

$$LAI = \frac{\log_e \left(\frac{L_c}{L_o} \right)}{k} \cos \theta \quad (7)$$

where, Θ is the sun zenith angle, k = canopy light extinction coefficient. A k value of 0.525 is used for mangrove stands (Green et al., 2014).

LAI is calculated in two steps: first determine the enhanced vegetation index (EVI) shown in Eq. (8) and then calculate LAI using the equation proposed by Boegh et al. (2002) and shown in Eq. (9). EVI was developed as a satellite vegetation product for the Moderate Resolution Imaging Spectroradiometer (MODIS) (Huete et al., 1999). EVI has high sensitivity in high biomass regions while

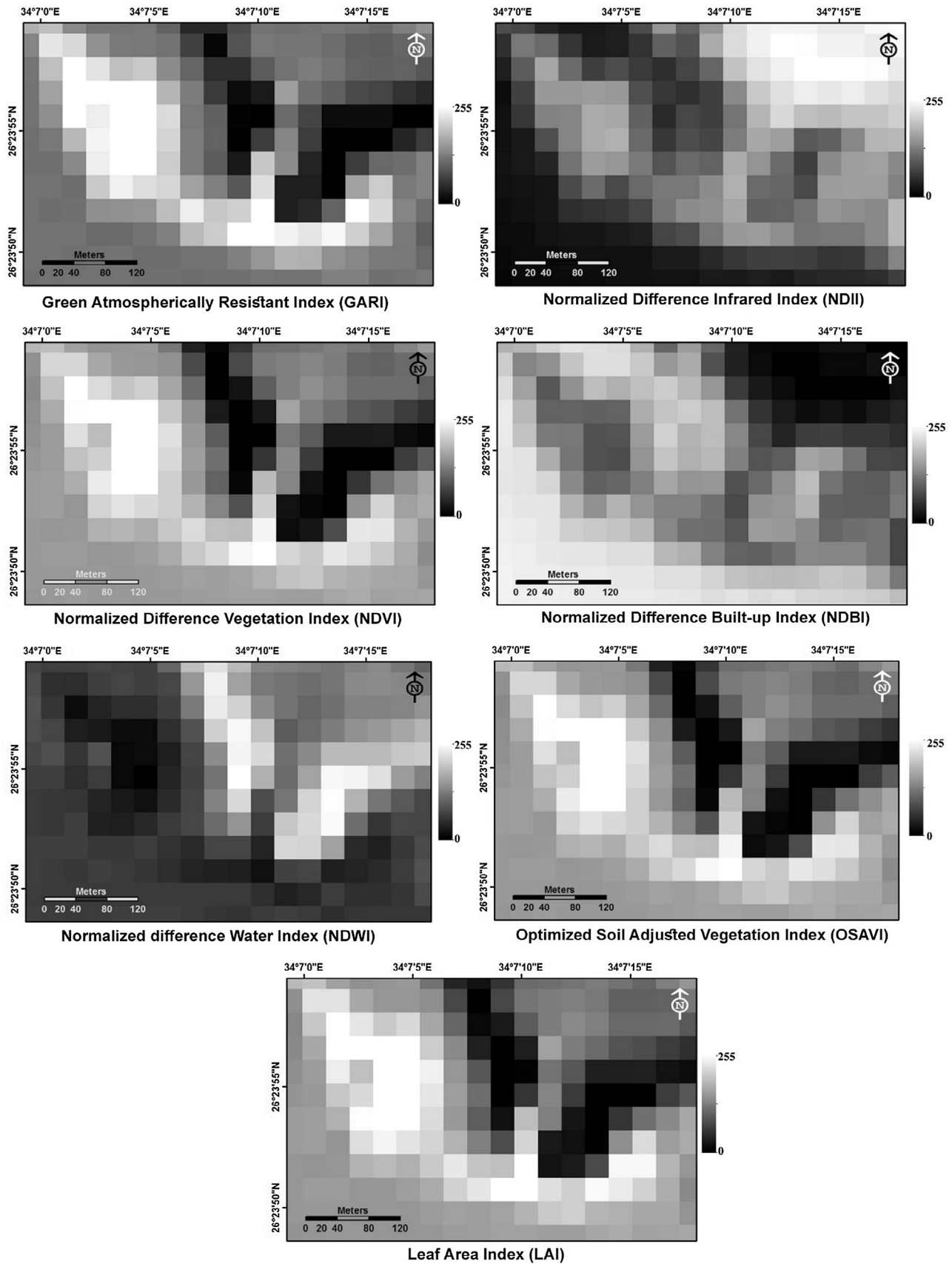


Fig. 4. Seven Vegetation Index layers rescaled for values between 0 and 255.

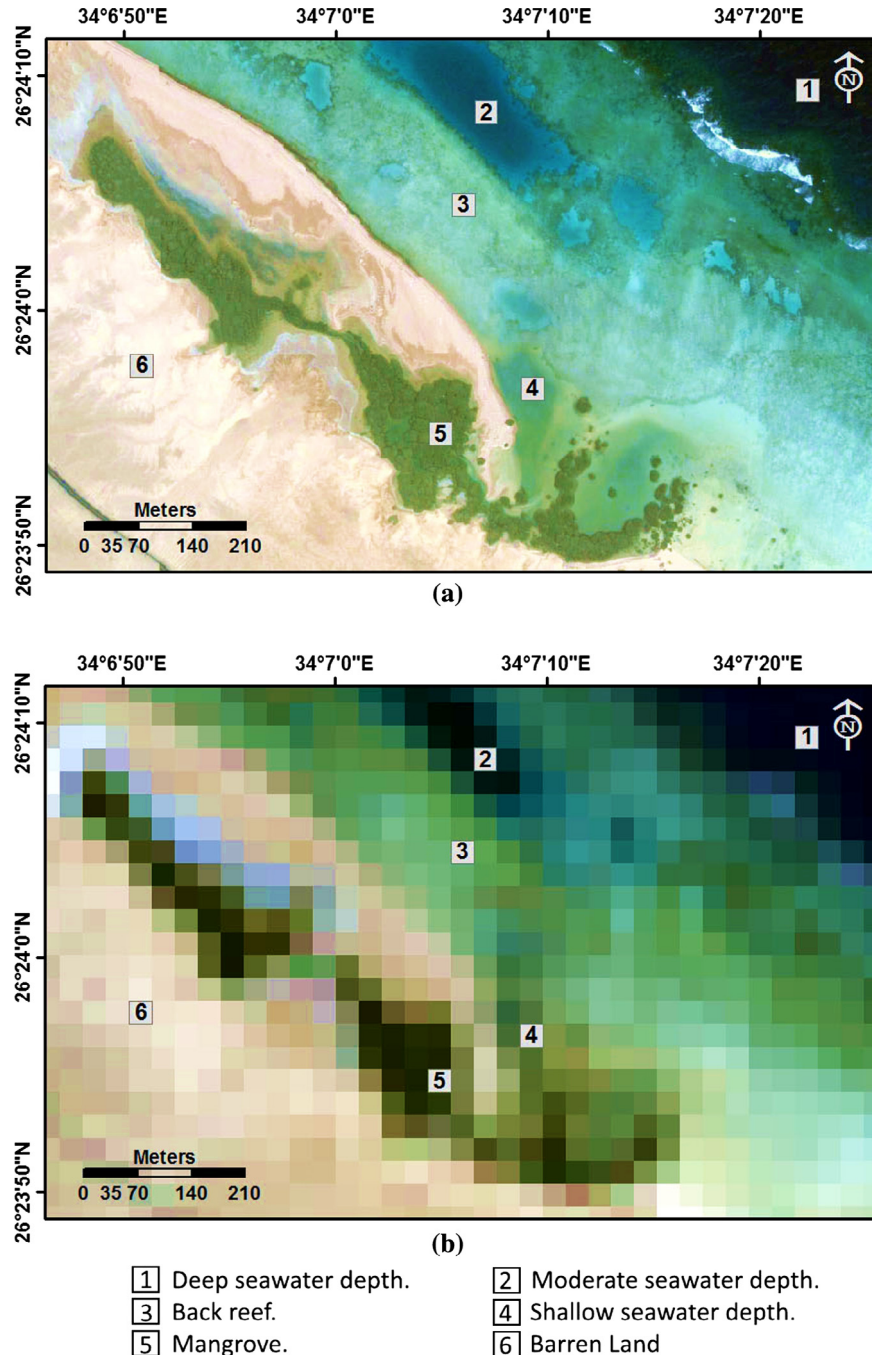


Fig. 5. Training set sites. (a) GeoEye image (bands 3, 2 and 1) and (b) Landsat 8 image (bands 4, 3 and 2).

minimizing soil and atmosphere influences. It is calculated using NIR, red and blue bands.

$$EVI = 2.5 \cdot \frac{(NIR - Red)}{(NIR + 6 \cdot Red - 7.5 \cdot Blue + 1)} \quad (8)$$

$$LAI = (3.618 \cdot EVI - 0.118) \succ 0 \quad (9)$$

The seven vegetation index layers (NDVI, NDII, LAI, GARI, OSAVI, NDBI, NSWI) were rescaled for values between 0 to 255, as shown in Fig. 4, and then stacked together into one image (a 7-index image).

3. Building a spectral library based on the index image

Unmixing algorithms is applied to the multispectral remote sensing image data to discriminate, classify, identify as well as quantify materials present in the image. One of most important parameters that affects the unmixing classification accuracy is the identification of pure signatures for each class in the image and saving it to a spectral library. The spectral library is then used in the unmixing classification process.

To build a spectral library for the study area, a sub-meter accuracy Magellan GPS with differential capability was attached to notebook computer loaded with an orthorectified Landsat 8 image of the area. The base station was placed on the roof of a building in

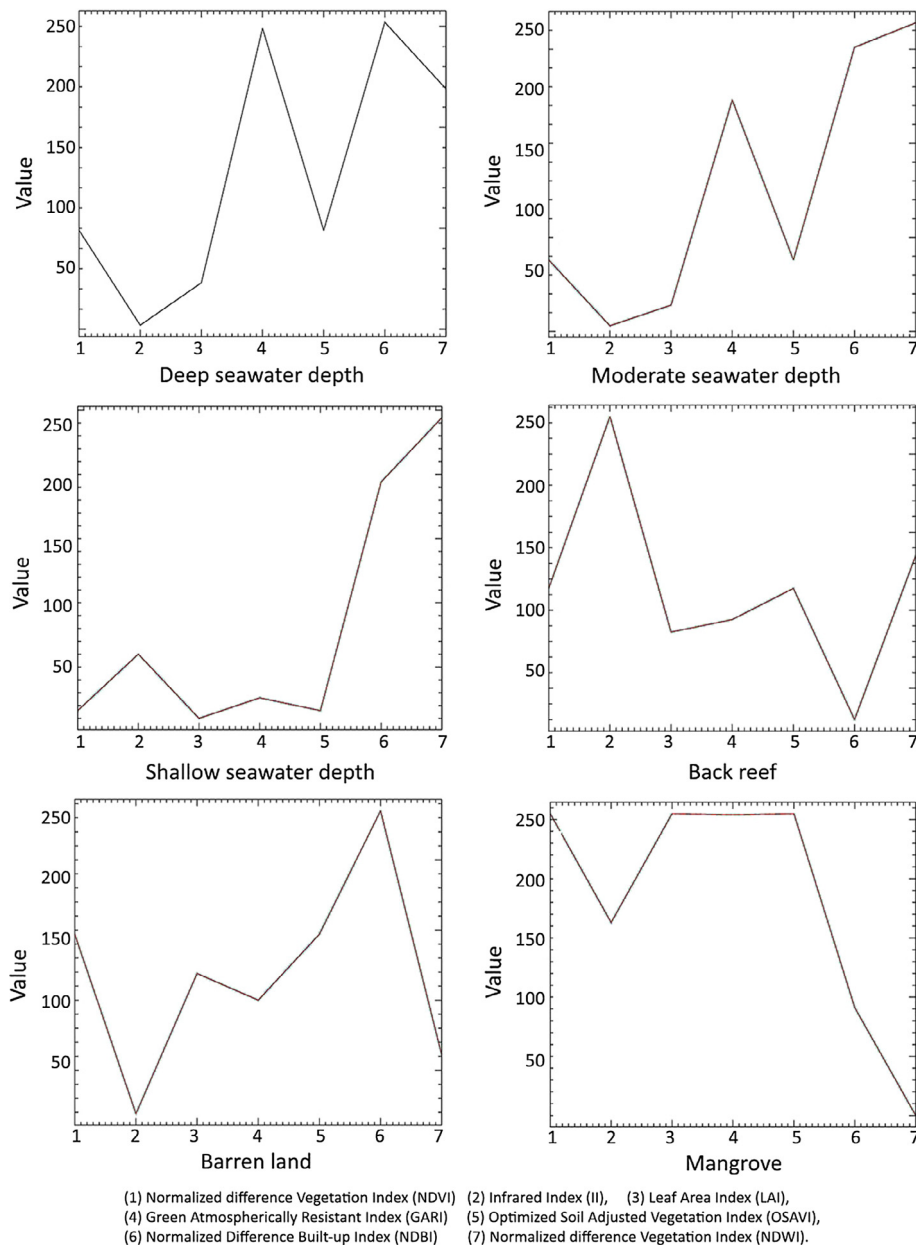


Fig. 6. Spectral reflectance curves for deep, moderate and shallow water, back reef, barren land and mangrove.

the city of Safqa. Land cover classes were identified in the field coincident with Landsat overpass. The training sites were 30 m × 30 m to coincide with the IFOV of Landsat 8. The training sets were chosen to be at the center of 90 m × 90 m area homogeneously covered by a land cover type.

ENVI (ver. 5.1) image processing software was used to determine the spectral signature of each training set. Six homogeneous spectral signatures representing the following cover types were identified: deep seawater, moderate seawater depth, shallow seawater, back reef, barren land and mangrove. The location of the training sets is shown in Fig. 5 and the spectral curves are shown in Fig. 6.

4. Seven index image unmixing analysis and mangrove canopy cover estimate

Many researchers found linear spectral unmixing method yielded good results when used for image classification (Drake

and white, 1991; Hu et al., 1999; Asner and Heidebrecht, 2002; Dobigeon et al., 2008). The unmixing algorithm was based on the following assumptions:

- Each IFOV may represent one land cover type (i.e., a pure IFOV or a mixed IFOV).
- The spectrum of the pure IFOV for a land cover is assumed to match the spectrum of that land cover type in the reference spectral library.
- The spectrum of mixed IFOV is a linear combination of the spectrum of the land covers present within the IFOV.

A linear spectral unmixing model was used to determine relative abundances of land cover types in the Abu Hamrah al Bahray area using the 7-index image and the land cover type spectral library. The unmixing result in each IFOV from each model was accepted only if it agreed with the following constraint:

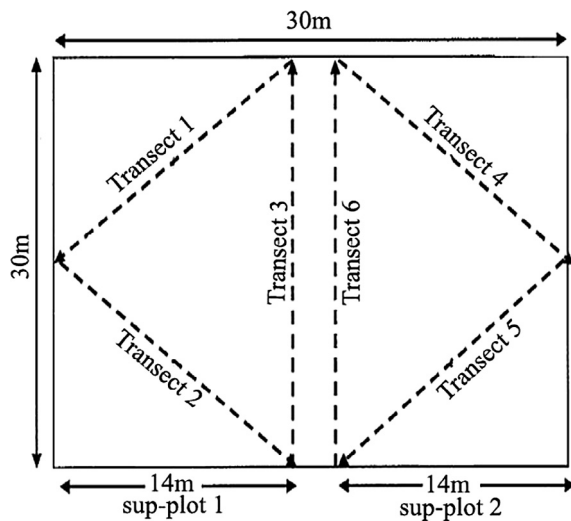


Fig. 7. Schematic diagram of a sample plot size with diamond-shaped layout transect for canopy cover measurements.

$$0 \leq f_r \leq 1$$

where, f_r is the estimated abundance fraction of each class.

5. Field measurement of mangrove canopy

During the period 25–30 July 2013, the mangrove canopy cover was measured by using a densitometer. The cover estimates generated using the densitometer were based on an evaluation of cover features collected at sample points evenly-spaced along transects. Sampling plots 30 m by 30 m in size were used. This plot size was found to be suitable for the size of the mangrove stands in the study area. The GPS attached to a laptop with an orthorectified Landsat 8 image was used for real-time in situ plot demarcation. The modified diamond shape plot was laid out using meter tapes to guide the recorder in the direction of the line as shown in Fig. 7.

Mangrove canopy cover measurements were carried out in the plots by walking along each transect and using the densitometer and recording, whether the canopy reading was open sky or vegetation, for every meter. We then used the consolidated canopy densitometer readings to determine canopy cover using Eq. (9):

$$C = \left(\frac{N_c}{N_r} \right)^* 100 \quad (9)$$

where:

C = canopy cover %.

N_c = number of readings indicating leaf vegetation.

N_r = total number of readings.

6. Results and discussion

The relative abundance of mangrove canopy in the Abu Hamrah al Bahray area is shown in Fig. 8. By comparing the data calculated by the unmixing technique with those done by observation, it was found that mangrove canopy cover data was, generally, lower than estimated. Therefore, the model required calibration.

The linear regression-calibration method has been suggested by several researchers (Prentice, 1982; Carroll and Stefanski, 1990; Hardin and Carroll, 2003). In order to develop the regression-calibration model for calculating the mangrove canopy cover using the unmixing classification process, we did the following: (1) Mangrove canopy coverage was measured at 35 sampling plots shown in Fig. 8 using the densitometer, (2) the measured canopy cover was linearly fit against data calculated from the unmixing model shown in Fig. 9. The regression-calibration model was built by using Microcal Origin software (ver. 5). The regression parameter values: standard errors, correlation coefficient (R), standard deviation, number of points used in the fit (N) and the p -value (probability that $R = 0$) showed the strong linear relationship between the observed and calculated data. The calibration model is given by Eq. (10).

$$\text{Mangrove Crop\%} = 19.58562 + (0.78268^* \text{ Unmixed Mangrove Fraction}) \quad (10)$$

The comparison between observed, calculated and calibrated mangrove canopy of Abu Hamrah al Bahray showed a good match between calibrated and observed data, as shown in Fig. 10.

In order to validate the seven index approach for estimating the mangrove canopy, it was applied to another stand of mangrove trees along the Egyptian Red Sea coast. The site chosen was the south Wadi Masturah grove. Twenty-six sampling plots were made in the mangrove and canopy was measured using a densitometer.

A linear spectral unmixing model was used to determine the relative abundance of the mangrove canopy. The model used the

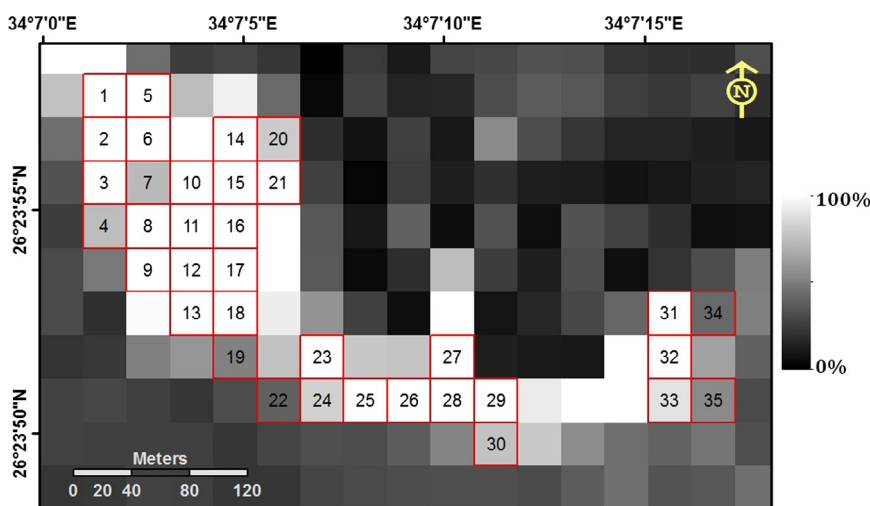


Fig. 8. Relative abundance of mangrove canopy overlaid by mangrove canopy in sampling grid.

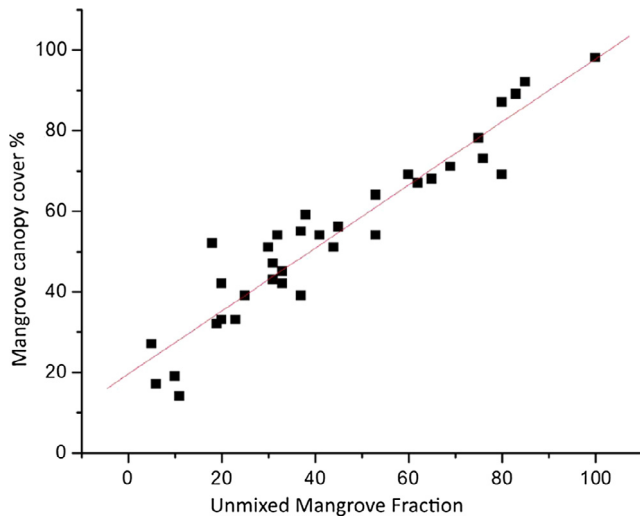


Fig. 9. Relationship between mangrove canopy cover and unmixed mangrove fraction calculated from the index image of the study area.

land cover spectral library developed for the Abu Hamrah al Bahray area because land cover of the two areas is similar. The resulting mangrove fraction model, shown in Fig. 11, was used to calculate the mangrove canopy cover of the sampling plots of Wadi Masturah. The values were then calibrated using the linear regression-calibration model shown in Table 1.

The square root of the variance of the errors (RMSE) was used to estimate how close the results of the new approach are to the observed data. RMSE is a good indicator of how accurately the model estimate or predicts. It is calculated by using Eq. (11):

$$RMSE = \sqrt{\frac{1}{N} \sum_{i=1}^N (X_0 - X_E)^2} \quad (11)$$

where, N is the number of observations, X_0 is the observed value and X_E is the value estimated by the model.

The RMSE for the estimated mangrove canopy of South Wadi Mastura mangrove was estimated to 4.9% meaning that the accuracy of mapping mangrove canopy using the new approach was approximately 95%. The success of the approach can be also

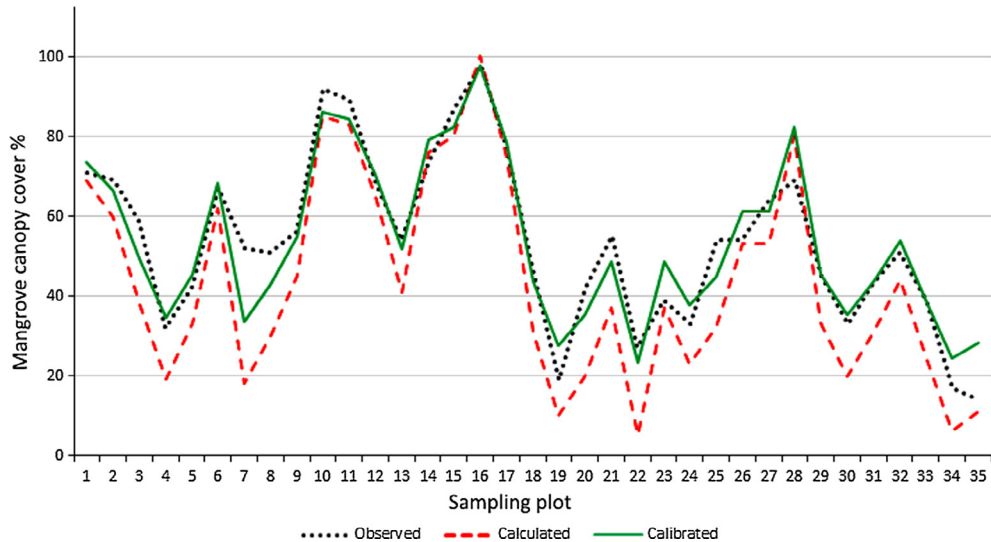


Fig. 10. Observed, calculated and calibrated mangrove canopy cover.

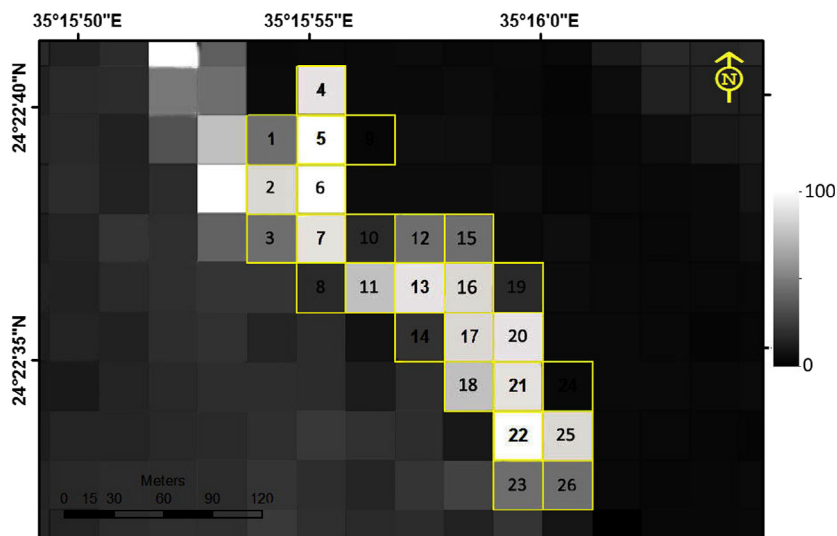


Fig. 11. Relative abundances of mangrove canopy in the South Wadi Mastura mangrove calculated by using the linear spectral unmixing model.

Table 1

Observed, calculated and calibrated values of mangrove canopy cover estimated using field surveys and Landsat 8.

ID_No	Observed	Calculated	Calibrated
1	21	4	23
2	47	38	49
3	23	6	24
4	46	37	49
5	84	82	84
6	79	79	81
7	60	51	60
8	18	2	21
9	20	2	21
10	16	7	25
11	28	9	27
12	23	6	24
13	47	33	45
14	15	3	22
15	17	2	21
16	41	29	42
17	36	23	38
18	26	7	25
19	11	1	20
20	52	42	52
21	56	50	59
22	27	8	26
23	12	1	20
24	5	2	21
25	45	33	45
26	18	1	20

shown by plotting the observed data against the data estimated by the new approach, as shown in Fig. 12.

On the other hand, Susan et al. (2011) evaluated the capability of using of 20 vegetation indices in measuring fractional vegetation

cover of Esfahan Desert, Iran. The vegetation indices were: NDVI, NDII, Modified Triangular Vegetation Index 2 (MTVI1), Modified Triangular, Vegetation Index 2 (MTVI2), Difference Vegetation Index (DVI), Soil-adjusted Vegetation Index (SAVI), Specific Leaf Area Vegetation Index (SLAVI), Green Normalized Difference, Vegetation Index (GNDVI), Transformed Vegetation Index (TVI), Simple Ratio Index (SR), Infrared Percentage Vegetation Index (IPVI), Simple Ratio Index (SR), Corrected Simple Ratio Index (SRc), Modified Simple Ratio Index (MSR), Ratio Difference Vegetation Index (RDVI), Non-Linear Index (NLI), Optimized Soil Adjusted Vegetation Index (OSAVI), Modified Soil Adjusted Vegetation Index (MSAVI) and Canopy Index (CI), Normalized Canopy Index (NCI). They measured the vegetation cover fraction in the field and then estimated its linear relationship with the vegetation indices at the IFOV level. The correlation between every vegetation indice and vegetation cover fraction was assessed and used as an indicator for the accuracy of the regression model in prediction of the vegetation cover fraction as shown in Table 2. DVI showed the highest linear correlation coefficient with a value of 0.8170. This indicated that the maximum accuracy that could be obtained by using any of these twenty vegetation indices would not exceed 82%.

The approach was used for mangrove demarcation and inventory for the mangrove stands within our study area. Mangroves exist as a small stands in six locations shown in Fig. 13:

- Abu Hamrah al Bahray
- Sharm Al Bahary
- Sharm Al Qibli
- Marsa Shajra
- Wadi Masturah (80 km south of Marsa Alam)
- Al-Qulaan (85 km south of Marsa Alam)

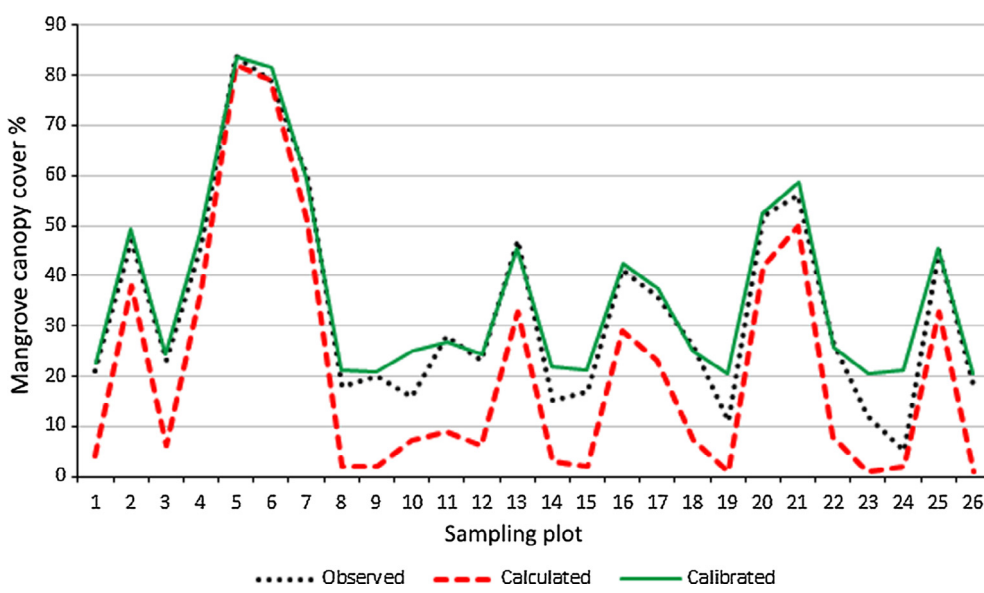


Fig. 12. Observed, calculated and calibrated mangrove canopy cover of South Wadi Mastura mangroves.

Table 2

Correlation Coefficient between Vegetation Indices and Vegetation Cover Fraction (Susan et al., 2011).

Vegetation index	SAVI	MSR	IPVI	RDVI	DVI	GNDVI	NDVIc	NDVI	SRc	SR
Correlation coefficient	0.720	0.723	0.719	0.798	0.817	0.570	0.674	0.719	0.765	0.727
Vegetation index	NCI	CI	SLAVI	NDII	MTVI2	MTVI1	TVI	NLI	MSAVI	OSAVI
Correlation coefficient	0.195	0.170	0.699	0.503	0.555	0.426	0.588	0.345	0.710	0.719

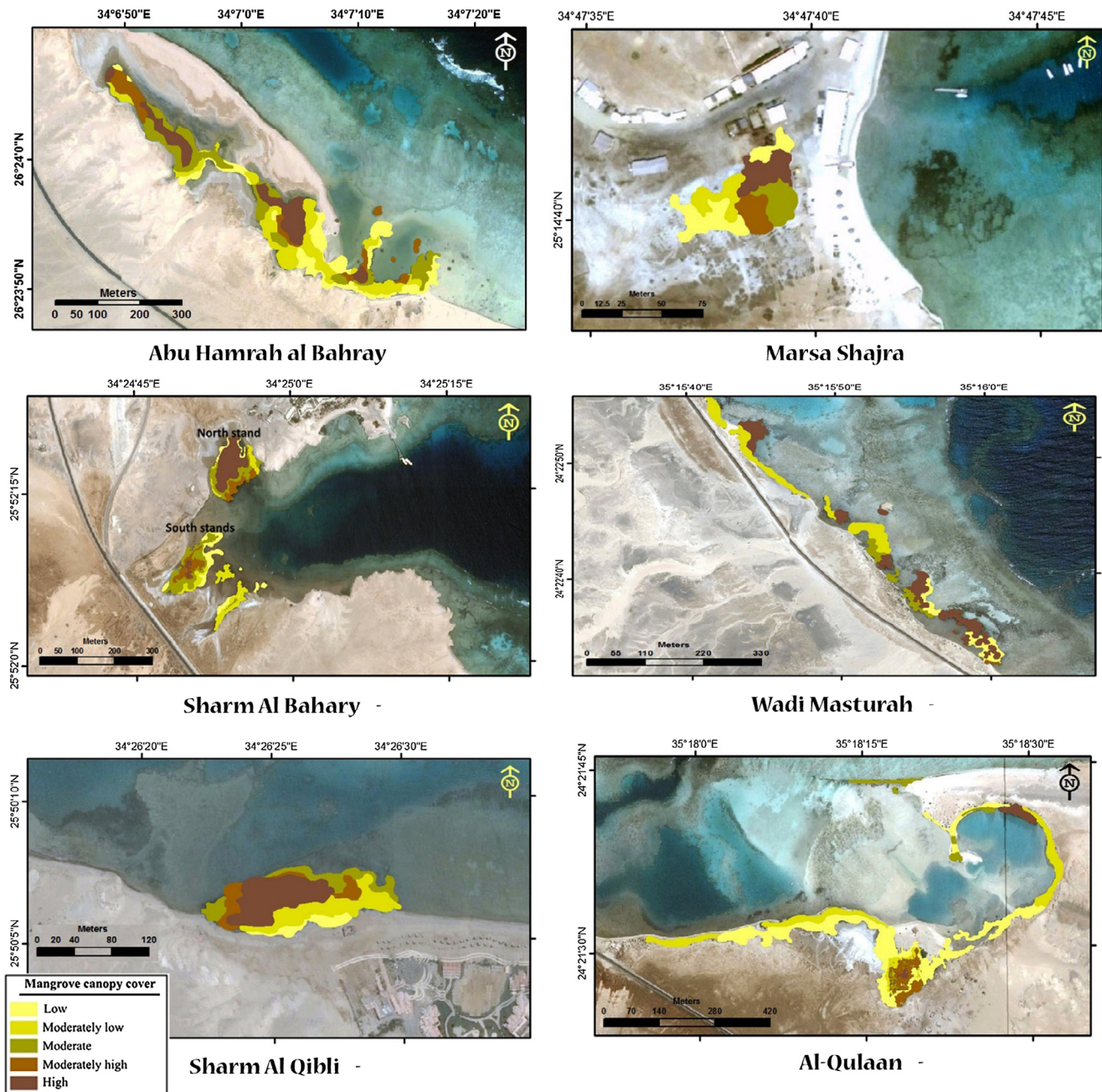


Fig. 13. Mangrove demarcation and inventory for mangrove stands.

7. Conclusions

By incorporating several vegetation indices, it is possible to accurately map the amount of vegetation cover of sparsely planted mangrove using Landsat 8 imagery. While some mangrove grove stands are large and dense, most along Egypt's Red Sea coast are small and sparse and so would be missed by Landsat 8. This is because most of the IFOVs would be a mix of vegetation, soil, branches and shadow. This research proved that a novel approach to improve the accuracy of mapping mangrove canopy using seven indexes (the Normalized Difference Vegetation Index, the Infrared Index, the Leaf Area Index, the Green Atmospherically Resistant Index, the Optimized Soil Adjusted Vegetation Index, the Normalized Difference Built-up Index and the Normalized Difference Water Index) worked. Results demonstrate that the accuracy of mapping mangrove was improved using this new technique.

Acknowledgements

This work was supported by the Egyptian Ministry for Scientific Research, Science and Technological Development Fund (STDF), Project ID: 5515 entitled “Locating Suitable Mangrove Plantation Sites Between El Quseir and Marsa Alam Using Remote Sensing and GIS”.

References

- Asner, G., Heidebrecht, K., 2002. Spectral unmixing of vegetation, soil and dry carbon cover in arid regions: comparing multispectral and hyperspectral observations. *Int. J. Remote Sens.* 23 (19), 3939–3958.
- Boegh, E., Soegaard, H., Broge, N., Hasager, C., Jensen, N., Schelde, K., Thomsen, A., 2002. Airborne multi-spectral data for quantifying leaf area index, nitrogen concentration and photosynthetic efficiency in agriculture. *Remote Sens. Environ.* 81 (2–3), 179–193.

- Carroll, R., Stefanski, L., 1990. Approximate quasi such as likelihood estimation in models with surrogate predictors. *J. Am. Stat. Assoc.* 85, 652–663.
- Dobigeon, N., Tourneret, J., Chang, C., 2008. Semi-supervised linear spectral unmixing using a hierarchical bayesian model for hyperspectral imagery. *Signal Process., IEEE Trans.* 56 (7), 2684–2695.
- Drake, N., White, K., 1991. Linear mixture modeling of landsat thematic mapper data for mapping the distribution and abundance of gypsum in the Tunisian Southern. *Spatial Data* 2000, 168–177 (Remote Sensing Society).
- English, S., Wilkinson, C., Baker, V., 1997. Survey Manual for Tropical Marine Resources. Australian Institute of Marine Science, p. 341.
- Gitelson, A., Kaufman, Y., Merzylak, M., 1996. Use of a green channel in remote sensing of global vegetation from EOS-MODIS. *Remote Sens. Environ.* 58, 289–298.
- Green, E., Mumby, P., Edwards, A., Clark, C., 2014. Remote Sensing Handbook for Tropical Coastal Management <http://www.unesco.org/csi/pub/source/rs.htm>. (Accessed 26/12/2014).
- Hardin, J., Carroll, R., 2003. Measurement error, GLMs, and notational conventions. *Stata J.* 3 (4), 328–340.
- Hardisky, M., Klemas, V., Smart, R., 1983. The influence of soil salinity, growth form and leaf moisture on the spectral radiance of *Spartina alterniflora* canopies. *Photogrammetric Eng. Remote Sens.* 48 (1), 77–84.
- Huete, A., Justice, C., van Leeuwen, W., 1999. MODIS vegetation index (MOD13) algorithm theoretical basis document. NASA Goddard Space Flight Center, http://modis.gsfc.nasa.gov/data/atbd/atbd_mod13.pdf, 120p.
- Hu, Y., Lee, H., Scarpace, F., 1999. Optimal linear spectral unmixing. *Geosci. Remote Sens., IEEE Trans.* 37 (1), 639–644. <http://dx.doi.org/10.1109/36.739139>.
- Prentice, R., 1982. Covariate measurement errors and parameter estimation in failure time regression models. *Biometrika* 69, 331–342.
- Rondeaux, G., Steven, M., Baret, F., 1996. Optimization of soil adjusted vegetation indices. *Remote Sens. Environ.* 55, 95–107.
- Rouse, W., Haas, H., Schell, A., Deering, W., 1974. Monitoring vegetation systems in the Great Plains with ERTS. In: Freden, S.C., Mercanti, E.P., Becker, M. (Eds.), *Third Earth Resources Technology Satellite-1 Symposium, Volume I: Technical Presentations*, NASA SP-351. NASA, Washington, DC, pp. 309–317.
- Sims, A., Gamon, A., 2003. Estimation of vegetation water content and photosynthetic tissue area from spectral reflectance: a comparison of indices based on liquid water and chlorophyll absorption features. *Remote Sens. Environ.* 84, 526–537.
- Susan, B., Behzad, R., Mehdi, S., Alireza, S., Masoud, N., 2011. Comparison the accuracies of different spectral indices for estimation of vegetation cover fraction in sparse vegetated areas. *Egypt. J. Remote Sensing Space Sci.* 14, 49–56.
- Small, C., 2004. The landsat ETM+ spectral mixing space. *Remote Sens. Environ.* 93, 1–17.
- Zha, Y., Gao, G., Ni, S., 2003. Use of normalized difference built-up index in automatically mapping urban areas from TM imagery. *Int. J. Remote Sens.* 24 (3), 583–594.